HHS Public Access

Author manuscript

Nat Med. Author manuscript; available in PMC 2014 April 01.

Published in final edited form as:

Nat Med. 2013 October ; 19(10): 1281–1287. doi:10.1038/nm.3288.

Autophagy regulates endothelial cell processing, maturation and secretion of von Willebrand factor

Takehiro Torisu[1,*], **Kumiko Torisu**[1,*], **In Hye Lee**[1], **Jie Liu**[1], **Daniela Malide**[2], **Christian A. Combs**[2], **Xufeng S. Wu**[3], **Ilsa I. Rovira**[1], **Maria M. Fergusson**[1], **Roberto Weigert**[4], **Patricia S. Connelly**[5], **Mathew P Daniels**[5], **Masaaki Komatsu**[6], **Liu Cao**[7], and **Toren Finkel**[1]

[1] Center for Molecular Medicine, NHLBI, NIH Bethesda, MD 20892

[2] Light Microscopy Core, NHLBI, NIH Bethesda, MD 20892

[3] Cell Biology and Physiology Center, NHLBI, NIH Bethesda, MD 20892

[4] Intracellular Membrane Trafficking Unit, NIDCR, NIH Bethesda, MD 20892

[5] Electron Microscopy Core Facility, NHLBI, NIH , Bethesda, MD 20892, USA

[6] Laboratory of Frontier Science, Tokyo Metropolitan Institute of Medical Sciences, Tokyo, Japan

[7] Key Laboratory of Medical Cell Biology, China Medical University, Shengyang, 110001, China

Abstract

Endothelial secretion of von Willebrand factor (VWF) from intracellular organelles known as Weibel-Palade bodies (WPBs) is required for platelet adhesion to the injured vessel wall. Here, we demonstrate that WPBs are in some cases found near or within autophagosomes and that endothelial autophagosomes contain abundant VWF protein. Pharmacological inhibitors of autophagy, or knockdown of the essential autophagy genes Atg5 or Atg7, inhibits the *in vitro* secretion of VWF. Furthermore, while mice with an endothelial specific deletion of Atg7 have normal vessel architecture and capillary density, these animals exhibit impaired epinephrine-stimulated VWF release, reduced levels of high molecular weight VWF multimers and a corresponding elevation of their bleeding times. Endothelial deletion of Atg5 or pharmacological inhibition of autophagic flux results in a similar *in vivo* alteration of hemostasis. Thus, autophagy regulates endothelial VWF secretion and transient pharmacological inhibition of autophagic flux may be a useful strategy to prevent thrombotic events.

Address Correspondence: Toren Finkel Center for Molecular Medicine Bldg 10/CRC 5-3330 Bethesda, MD 20892 T: 301-402-4081 finkelt@nih.gov.

*These authors contributed equally

Author Contributions: T.T. and K.T designed, performed and analyzed the experiments and aided in writing the manuscript. I.H.L, J.L, I.I.R, M.M.F., L.C. contributed to the completion of various experiments. D.M., C.A.C., X.S.W, R.W., P.S.C., M.P.D. aided in specialized imaging procedures, M.K. provided valuable reagents and advice, and T.F. helped conceive the study, supervised the research and contributed to the writing the manuscript.

Introduction

While macroautophagy, herein simply termed autophagy, plays an indispensible role in the intracellular degradation of proteins and organelles, there is growing evidence that also implicates this process in protein secretion[1-4]. This link includes a role for autophagy in regulating unconventional secretion of Acb1 in yeast [5,6] and interleukin-1β (IL-1β) in mammalian cells[7]. There is also evidence that autophagy regulates conventional secretory pathways. For instance, the constitutive secretion of IL-6 and IL-8 from senescent cells appears to involve the formation of a specialized cellular domain termed the TOR-autophagy spatial coupling compartment (TASCC). This compartment is directly adjacent to the trans Golgi network and is enriched for both signaling proteins such as mTOR, as well as for autophagic vacuoles[8]. Finally, there are a growing number of studies suggesting a connection between components of the autophagy machinery and the regulated secretion of intracellular lysosomes or granules. For instance, deficiency in specific essential autophagy proteins appear to impair regulated secretion from the intestinal Paneth cell[9,10], bone marrow derived mast cells[11], pancreatic β-cells[12,13], melanocytes[14], osteoclasts[15] and vestibular epithelial cells[16].

Exocytosis from endothelial cells represents one of the first lines of defense following vascular injury. Specific secretory granules within the endothelial cell known as Weibel-Palade bodies (WPBs) contain numerous biologically active molecules, although von Willebrand factor (VWF) is by far the most abundant[17,18]. Indeed, VWF is required for formation of WPBs[19,20], and heterologous expression of VWF in non-endothelial cells can induce the formation of WPB-like structures[21,22]. Once secreted, VWF multimers can assemble into long strings that can become tethered to the underlying connective tissue while simultaneously ensnaring circulating platelets. This secretion and subsequent string formation is essential for appropriate hemostasis after injury. Impaired production, processing or secretion of VWF results in the clinical syndrome known as von Willebrand disease, recognized as the most common inherited bleeding disorder[23].

The production of WPBs is a complex process involving dimerization and disulfide bond formation in the endoplasmic reticulum followed by furin-dependent cleavage in the Golgi complex[18,24]. The VWF multimers that form can then be folded, in a pH-sensitive fashion, into tubular structures[25,26]. While structural mutations in VWF can lead to defects in multimer formation or tubulation, relatively little is known about what other cellular processes regulate the number, pH or secretory potential of WPBs. Here, we demonstrate that autophagy plays a critical role in the biology of WPBs and regulates the *in vitro* and *in vivo* release of VWF.

Results

Proximity of endothelial WPBs to autophagosomes

While there is a growing understanding of the molecular and biological role of autophagy, the role this process plays within the vasculature is poorly understood. In an effort to better understand how autophagy might contribute to vessel homeostasis, we analyzed electron micrographs of primary human umbilical vein endothelial cells (HUVECs). Both WPBs and

autophagosomes have distinctive appearance by electron microscopy, with the former exhibiting a classical cigar shaped appearance and the latter being an intracellular organelle often filled with diverse cellular contents surrounded by a unique double membrane structure. Surprisingly, we noted that within endothelial cells, WPBs and autophagosomes were often found in close proximity. Moreover, we noted multiple instances in which a WPB appeared to be very near and actively fusing with an autophagosome (Fig. 1a and Supplemental Fig. 1a). Examination of the contents of autophagosomes also revealed the presence of what appeared to be wholly or partially intact WPBs, clearly identifiable by their unique shape and internal striations running parallel to their long axis (Fig. 1b). To further pursue these observations we performed additional immunogold labeling coupled with electron microscopy analysis to assess the distribution of VWF within endothelial cells. These studies revealed that as expected, VWF was present at high abundance within mature WPBs (Fig. 1c). VWF was also found within cisternae of the endoplasmic reticulum (Supplemental Fig. 1b). In addition, we observed a significant amount of VWF within mature autophagosomes. This immunogold labeled VWF signal appeared to be composed of both free protein, as well as, what appeared to be wholly or partially intact WPBs (Fig. 1d and Supplemental Fig. 1c-e). Analyzing 30 random section containing several hundred autophagosomes revealed that 17 % of the autophagosomes had no detectable VWF signal (48/279), 42% (117/279) of the autophagosomes had a moderate amount of VWF (1-10 immunogold particles) and 41% (114/279) of the autophagosomes had a robust signal for VWF (>10 immunogold particles per autophagosome).

The electron microscopic observations suggested that autophagosomes, and by extension autophagy, might somehow modulate VWF levels or secretion. Autophagosome formation requires that the cytosolic form of LC3 (LC3-I) be conjugated in an Atg5 and Atg7 dependent fashion to form the lipidated LC3-II species[27]. Based on these past observations, we next sought to analyze the distribution of VWF and LC3 (Atg8) using super resolution structured illumination microscopy. These images revealed the expected cigar shaped WPB morphology and the classical spherical punctae of lipidated LC3-II (Fig. 1e). Within endothelial cells, super resolution microscopy revealed that endogenous VWF and LC3 were clearly separable. Nonetheless, at any given time, a substantial fraction of WPBs were closely associated with a LC3 signal (37/224 WPBs or 16.7%) with a smaller percentage of WPBs (7/224 or 3.2%) appearing to be surrounded by a structure consistent with a LC3-coated autophagosome (Fig. 1e and Supplemental Movie 1). A separate analysis using confocal microscopy came to a similar conclusion, namely that a substantial fraction (approximately 30%) of intracellular LC3 and VWF spots had a centroid to centroid distance of less than 1.5 μm (Supplemental Fig. 2a). This association was significantly higher than predicted by chance alone (Supplemental Fig. 2b). Finally, using two color confocal live cell imaging, we could capture in real time, the apparent direct interaction of a LC3-GFP autophagosome with a VWF-mCherry positive WPB (Fig. 1f&g). Nonetheless, additional dual-color (LC3-mCherry and VWF-GFP) or single color (LC3-GFP) TIRF imaging suggested these interactions were rare and that under normal circumstances, autophagosomes do not appear to directly fuse with the plasma membrane (Supplemental movie 2&3).

Autophagy regulates *in vitro* VWF secretion

To begin to address whether autophagy modulates VWF biology, we performed lentiviral shRNA mediated knockdown of Atg7 in human endothelial cells. In Atg7 knockdown cells, Western blot analysis confirmed a significant reduction in Atg7 expression (Fig. 2a). Assessment of autophagic flux often relies on the simultaneous measurements of the level of expression of the multidomain, signaling adaptor protein p62/A170/SQSTM1, hereafter referred to simply as p62, along with the ratio of LC3-II to LC3-I. A rise in p62 levels and a fall in LC3-II are consistent with impaired autophagic flux[28,29]. As expected, knockdown of the essential autophagy gene Atg7 had the expected effects on these well characterized markers of autophagic flux (Fig. 2a). We then asked whether knockdown of Atg7 altered the stimulated release of VWF. Using an ELISA-based method of the culture medium, we detected an increase in VWF secretion following stimulation with histamine or VEGF (Fig. 2b). In contrast, Atg7 knockdown cells had impaired ligand-stimulated release of VWF. We saw similar effects on VWF secretion using an alternative and independent method for knockdown of Atg7 that employed siRNA (Supplemental Fig. 3). The reduction in the stimulated release of VWF was further confirmed by direct Western blot analysis of the endothelial cell supernatant (Fig. 2c,d).

A recent report has suggested that disruption of autophagy might alter intracellular calcium signaling[30]. Given the central role of calcium in stimulated exocytosis from the endothelium, we wondered whether such a mechanism might explain our observations. Using a calcium sensitive fluorometric probe, we could not however detect significant differences in ligand-induced calcium transients between control and Atg7 knockdown cells (Fig. 2e). Similarly, other proximal signaling events such as extracellular regulated kinase (ERK) activation appeared to be unaffected by Atg7 knockdown (Supplemental Fig. 4).

We next sought to establish whether other genetic or pharmacological inhibitors of autophagy had similar effects. Knockdown of the essential autophagy gene Atg5 alone or in combination with Atg7 also inhibited VWF release (Fig. 2f, g and Supplemental Fig. 5a). Following histamine stimulation, the combined knockdown of Atg5 and Atg7 appeared slightly more effective than single knockdown of either Atg7 or Atg5 in blocking VWF secretion (Fig. 2g). Incubation of human endothelial cells with chloroquine or bafilomycin, two known inhibitors of autophagic flux, also resulted in a marked inhibition of ligand-stimulated VWF secretion (Fig. 2h). In contrast, knockdown of Atg5 or Atg7 did not appear to alter ligand-stimulated release of endothelin-1 from endothelial cells (Supplemental Fig. 5b). In addition, while knockdown of Atg6 (beclin 1) was quite effective in reducing Atg6 expression (Fig 2i), it had only a very modest effect on markers of autophagic flux (Supplemental Fig. 5c) and no significant effect on VWF secretion (Fig. 2j).

Autophagy is required for VWF protein maturation

We next sought to attempt to get a better understanding of why knockdown of an essential autophagy gene such as Atg7 might inhibit the secretion of VWF. Following synthesis, VWF undergoes a series of processing events in the ER and Golgi that eventually lead to maturation of the protein and incorporation into WPBs[31]. Using a quantitative ELISA-based method we determined that the total intracellular level of VWF protein was not significantly

different between control and Atg7 knockdown endothelial cells (Fig. 3a). Similar results were observed following knockdown of Atg5 or combined Atg5 and Atg7 knockdown (Supplemental Fig. 6a). We next sought to analyze whether differences might exist in the processing, maturation and secretion of VWF. The processing of VWF involves a furin-dependent proteoltyic cleavage within the trans-Golgi network with the pro-VWF precursor distinguishable from mature VWF based on electrophoretic mobility[32]. We observed that the steady state ratio of pro-VWF to mature VWF was significantly altered in Atg7 or Atg5 knockdown cell (Fig. 3b, c and Supplemental Fig. 6b). Consistent with a defect in VWF processing, we also noted a reduction in the number of mature WPBs observed in Atg7 knockdown cells (Fig. 3d). We saw similar reduction in WPBs in endothelial cells with either Atg5 knockdown or following pharmacological inhibition of autophagy using chloroquine or bafilomycin (Supplemental Fig. 7a, b). In contrast, knockdown of Atg6 did not alter the number of mature WPBs (Supplemental Fig. 7c). These results suggest that one explanation for our observation with Atg5 or Atg7 knockdown is that these strategies, while not altering overall VWF expression, appear to inhibit the processing and maturation of VWF into mature WPBs.

The formation of WPBs is believed to occur at the trans-Golgi network (TGN)[33] and autophagy is known to be critical for the homeostatic maintenance of both the ER and Golgi[34]. Furthermore, the pH of WPBs is known to be acidic and this low pH is essential for the shape of the WPBs, as well as VWF tubulation and function [26,35,36]. Using previously described methods[35], we were able to establish that WPBs within Atg7 knockdown cells exhibited a higher pH than WPBs found in control cells (Fig. 4a and Supplemental Fig. 8). Consistent with previous results[26], when assessed by confocal microscopy, this higher pH in Atg7 knockdown cells resulted in rounder and less rod-shaped WPBs (Fig. 4b, c). This also translated into a statistically significant reduction in the length of WPBs found in Atg7 knockdown cells (Fig. 4d). Similar observations were evident by electron microscopy where we observed that knockdown of Atg7 resulted in WPBs that were shorter, rounder and had less distinct tubulation (Fig. 4e).

To further assess whether in addition to a processing defect, there was also an effect of Atg7 on the secretion of mature WPBs, we employed a previously described system using live cell imaging of the secretion of a VWF-GFP chimeric fusion protein[37]. Expression of this tagged VWF results in assembly of WPBs containing the co-expressed fluorescently labeled VWF protein (Supplemental Fig. 9a). Consistent with the alterations in processing described above, the number of GFP-positive WPBs was reduced in cells where Atg7 was knockdown (Supplemental Fig. 9b) and the WPBs that formed, had an altered, more rounded morphology (Supplemental movies 4, 5). Using this system, in conjunction with total internal reflection fluorescence (TIRF) microscopy, we could monitor individual secretion events of GFP-positive WPBs that localized near the plasma membrane (Fig. 4f and Supplemental movies 4, 5). Our analysis demonstrated that knockdown of Atg7 resulted in reduced WPB secretion after histamine stimulation (Fig. 4g).

Autophagy regulates in vivo VWF release

In an effort to extend these observations to an *in vivo* situation, we conditionally deleted Atg7 within endothelial cells by crossing mice harboring Atg7 floxed alleles with transgenic mice expressing the previously described VE-Cadherin Cre recombinase[38]. Parental mice both of which bore the genotype $Atg7^{f/wt}$; VE-Cadherin Cre were crossed to generate offspring that were either $Atg7^{f/f}$; VE-Cadherin Cre (hereafter denoted as $Atg7^{endo}$) or $Atg7^{wt/wt}$; VE-Cadherin Cre (hereafter denoted as control). Given the relatively small contribution of endothelial cells to overall organ mass, we did not observe a significant reduction in Atg7 expression in the tissues and organs isolated from $Atg7^{endo}$ mice (Supplemental Fig. 10). In contrast, primary cultures of mouse endothelial cells isolated from $Atg7^{endo}$ mice exhibited the expected reduction in Atg7 expression (Fig. 5a). The residual expression of Atg7 in these cells may represent a combination of incomplete deletion with VE-Cadherin Cre, as well as potentially some degree of contamination of non-endothelial cells in these primary cultures. Nonetheless, this level of Atg7 expression was sufficient to induce a reduction in autophagic flux as evidenced by the LC3-I/II ratio and p62 levels (Fig. 5a). Conditional deletion of endothelial Atg7 did not alter VWF expression (Supplemental Fig. 11a). Similar to our observations employing knockdown of Atg7 in human endothelial cells, we did however observe a reduction in the number of mature WPBs in endothelial cells derived from $Atg7^{endo}$ mice (Fig 5b).

While conditional deletion of essential autophagy genes in tissues such as brain led to marked alterations in tissue homeostasis and early mortality[39,40], $Atg7^{endo}$ mice exhibited no obvious vascular phenotypes. Similarly, $Atg7^{endo}$ mice exhibited no increase in mortality over the first year of life (unpublished observations). Assessment of vascular density demonstrated that $Atg7^{endo}$ mice were indistinguishable from control animals (Fig. 5c). In addition, while autophagy has been implicated in angiogenesis[41,42], we saw no consistent or reproducible abnormalities in $Atg7^{endo}$ mice when post-natal retinal angiogenesis was assessed (Fig. 5d). Furthermore, the endothelium and underlying architecture of large vessels were similar in $Atg7^{endo}$ and control mice (Fig. 5e). We also observed no reduction in the level of VWF expression in $Atg7^{endo}$ mice either by immunohistochemical (Fig. 5e) or by Western blot analysis (Supplemental Fig. 11b).

We next asked whether $Atg7^{endo}$ mice exhibited defects in VWF secretion. In control mice, injection of epinephrine led to a significant rise in plasma VWF levels (Fig. 6a, fold increase: 1.5 +/− 0.04, n=27 mice, $p<0.001$ pre versus post). This increase in VWF in response to subcutaneous epinephrine injection is similar in magnitude to previous reports[43]. In contrast, $Atg7^{endo}$ mice failed to respond in a significant fashion to an epinephrine challenge (Fig. 6a, fold increase: 1.17 +/− 0.05, n=13 mice, p=NS pre versus post). This lack of stimulated epinephrine release was also evident in mice where Atg5 had been conditionally deleted again using VE-Cadherin Cre. Similar to $Atg7^{endo}$ mice, $Atg5^{endo}$ mice also failed to respond to epinephrine (Fig. 6a, fold increase: 1.13 +/− 0.07, n=9 mice, p=NS pre versus post). Neither $Atg5^{endo}$ mice nor $Atg7^{endo}$ mice had a significant reduction in basal VWF (Fig. 6a). Similarly, basal levels of circulating P-selectin levels were not altered between control and $Atg7^{endo}$ mice (Supplemental Fig. 12). To therefore further assess the role of autophagy in regulating basal VWF levels, we analyzed mice having a

complete, whole body knockout of Atg7. Previous studies demonstrated that these total body Atg7 knockout mice rarely survive for more than 48 hours after birth[44,45]. When we analyzed Atg7$^{-/-}$ mice shortly after delivery, we did note a reduction in plasma VWF when compared to wild type littermates, perhaps reflective of a more complete knockout in this model then can be achieved using conditional approaches (Fig. 6b).

We next sought to further characterize the physiological importance of Atg7 in VWF processing *in vivo*. Consistent with the observed *in vitro* deficit in VWF processing, we noted that on non-reducing gels, plasma VWF analyzed from Atg7^{endo} mice contained diminished levels of the biologically active, higher molecular weight multimers (Fig. 6c). Consistent with this reduction in high molecular weight VWF, coupled with the decrement in stimulated VWF release (Fig. 6a), we noted a significant increase in measured bleeding time when control mice were compared to Atg7^{endo} mice (Fig. 6d). Such differences occurred in the absence of any measurable differences in various hemostatic parameters (Supplemental Fig. 13). Furthermore, we did not see any obvious abnormalities in platelet morphology or platelet VWF levels that could have potentially contributed to the observed alterations in the measured bleeding time (Supplemental Fig. 14).

Given that one of the many effects for chloroquine is inhibition of autophagy and since this agent is approved for human usage, we next randomized mice to saline or chloroquine (CQ) injections. After 9 days, basal plasma VWF levels in CQ treated and vehicle treated mice were similar (Supplemental Fig. 15a). Nonetheless, direct assessment of hemostasis revealed that similar to Atg7^{endo} mice, pharmacological inhibition of autophagic flux resulted in a significant prolongation of bleeding time (Fig. 6e and Supplemental Fig. 15b).

Discussion

Our data suggests that knockdown or deletion of Atg5 or Atg7 results in the impaired *in vitro* and *in vivo* stimulated secretion of VWF. Interestingly, we and others have demonstrated that conditional deletion of Atg7 within the pancreatic β-cell leads to impaired secretion of insulin[12,13,46]. Similarly, impaired granular exocytosis is observed following disruption of autophagy within mast cells[11], the intestinal Paneth cell[9] and osteoclasts[15]. Thus, our current results, in conjunction with these past observations, suggest that in addition to its known role in intracellular recycling, autophagy plays a fundamental role in the regulated secretion that occurs in certain specialized cell types.

It is currently unclear in the case of mast cells, Paneth cells or osteoclasts exactly how autophagy regulates granule secretion[9,11, 15]. Our data suggests that autophagosomes and WPBs can directly interact and that VWF protein and WPB remnants appear to be found within autophagosomes. Recent evidence suggests that under certain conditions (e.g. starvation), autophagic vacuoles can actually be directly secreted by endothelial cells[47,48]. Consistent with our microscopy observations, proteomic analysis of these secreted endothelial autophagic vacuoles reveals they contain VWF[48]. Nonetheless, although our data suggests an interaction between autophagosomes and WPBs, this interaction is relatively rare when assessed by electron microscopy, super resolution microscopy or dual-color TIRF imaging. One intriguing possibility is that the observed interaction represents a

mechanism to remove damaged or dysfunctional WPBs, in a similar fashion to how mitophagy is thought to remove damaged mitochondria. How autophagosomes could potentially distinguish a normal from a damaged WPB is unclear, although in this regard, the basis of mitophagic selectivity also remains unresolved.

Finally, it is interesting to note that our observations may have important therapeutic implications. Our data suggests that chloroquine administration can increase the bleeding time of mice. This agent has many effects on cells since it can suppress the acidification of late endosomes, MVBs and lysosomes. The latter property results in the disruption of autophagic flux. Chloroquine is widely given for the treatment and prevention of malaria as well as for treatment of certain classes of autoimmune diseases. Interestingly, one known side effect of the drug is an increased risk for bleeding and the longer acting derivative hydroxychloroquine has been shown to be effective in humans as a prophylaxis against thromboembolic complications following surgery[49]. The mechanism for this protective effect of hydroxychloroquine is not well understood. Our data provides support to the notion that other agents that similarly target autophagic flux might also modulate VWF secretion. As such, targeted pharmacological inhibition of the autophagic pathway may provide a novel approach to reduce thrombus formation.

Supplementary Material

Refer to Web version on PubMed Central for supplementary material.

Acknowledgements

We are grateful to S. Gutkind (NIH) for help with primary endothelial cell isolation, T. Carter for the gift of the VWF-GFP plasmid, J. Lippincott-Schwartz for the LC3-mCherry plasmid and Y. Fitz for help on coagulation measurements. We thank Dr. Bernd Zinselmeyer (NINDS, NIH) for assistance with the spot cluster analysis and Christine A. Brantner for help with performing cryo-immunogold EM. This work was supported by NIH Intramural Funds. T.T. is a recipient of a JSPS Research Fellowship in Biomedical and Behavioral Research at NIH.

References

1. Pfeffer SR. Unconventional secretion by autophagosome exocytosis. J Cell Biol. 2010; 188:451–452. [PubMed: 20156968]
2. Abrahamsen H, Stenmark H. Protein secretion: unconventional exit by exophagy. Curr Biol. 2010; 20:R415–418. [PubMed: 20462486]
3. Manjithaya R, Subramani S. Autophagy: a broad role in unconventional protein secretion? Trends Cell Biol. 2011; 21:67–73. [PubMed: 20961762]
4. Deretic V, Jiang S, Dupont N. Autophagy intersections with conventional and unconventional secretion in tissue development, remodeling and inflammation. Trends Cell Biol. 2012; 22:397–406. [PubMed: 22677446]
5. Duran JM, Anjard C, Stefan C, Loomis WF, Malhotra V. Unconventional secretion of Acb1 is mediated by autophagosomes. J Cell Biol. 2010; 188:527–536. [PubMed: 20156967]
6. Manjithaya R, Anjard C, Loomis WF, Subramani S. Unconventional secretion of Pichia pastoris Acb1 is dependent on GRASP protein, peroxisomal functions, and autophagosome formation. J Cell Biol. 2010; 188:537–546. [PubMed: 20156962]
7. Dupont N, et al. Autophagy-based unconventional secretory pathway for extracellular delivery of IL-1beta. EMBO J. 2011; 30:4701–4711. [PubMed: 22068051]
8. Narita M, et al. Spatial coupling of mTOR and autophagy augments secretory phenotypes. Science. 2011; 332:966–970. [PubMed: 21512002]

9. Cadwell K, et al. A key role for autophagy and the autophagy gene Atg16l1 in mouse and human intestinal Paneth cells. Nature. 2008; 456:259–263. [PubMed: 18849966]
10. Cadwell K, et al. Virus-plus-susceptibility gene interaction determines Crohn's disease gene Atg16L1 phenotypes in intestine. Cell. 2010; 141:1135–1145. [PubMed: 20602997]
11. Ushio H, et al. Crucial role for autophagy in degranulation of mast cells. J Allergy Clin Immunol. 2011; 127:1267–1276. e1266. [PubMed: 21333342]
12. Ebato C, et al. Autophagy is important in islet homeostasis and compensatory increase of beta cell mass in response to high-fat diet. Cell Metab. 2008; 8:325–332. [PubMed: 18840363]
13. Jung HS, et al. Loss of autophagy diminishes pancreatic beta cell mass and function with resultant hyperglycemia. Cell Metab. 2008; 8:318–324. [PubMed: 18840362]
14. Ganesan AK, et al. Genome-wide siRNA-based functional genomics of pigmentation identifies novel genes and pathways that impact melanogenesis in human cells. PLoS Genet. 2008; 4:e1000298. [PubMed: 19057677]
15. DeSelm CJ, et al. Autophagy proteins regulate the secretory component of osteoclastic bone resorption. Dev Cell. 2011; 21:966–974. [PubMed: 22055344]
16. Marino G, et al. Autophagy is essential for mouse sense of balance. J Clin Invest. 2010; 120:2331–2344. [PubMed: 20577052]
17. Lowenstein CJ, Morrell CN, Yamakuchi M. Regulation of Weibel-Palade body exocytosis. Trends Cardiovasc Med. 2005; 15:302–308. [PubMed: 16297768]
18. Valentijn KM, Sadler JE, Valentijn JA, Voorberg J, Eikenboom J. Functional architecture of Weibel-Palade bodies. Blood. 2011; 117:5033–5043. [PubMed: 21266719]
19. Denis CV, Andre P, Saffaripour S, Wagner DD. Defect in regulated secretion of P-selectin affects leukocyte recruitment in von Willebrand factor-deficient mice. Proc Natl Acad Sci U S A. 2001; 98:4072–4077. [PubMed: 11274431]
20. Haberichter SL, et al. Re-establishment of VWF-dependent Weibel-Palade bodies in VWD endothelial cells. Blood. 2005; 105:145–152. [PubMed: 15331450]
21. Wagner DD, et al. Induction of specific storage organelles by von Willebrand factor propolypeptide. Cell. 1991; 64:403–413. [PubMed: 1988154]
22. Voorberg J, et al. Biogenesis of von Willebrand factor-containing organelles in heterologous transfected CV-1 cells. EMBO J. 1993; 12:749–758. [PubMed: 8440262]
23. Rodeghiero F, Castaman G, Dini E. Epidemiological investigation of the prevalence of von Willebrand's disease. Blood. 1987; 69:454–459. [PubMed: 3492222]
24. Metcalf DJ, Nightingale TD, Zenner HL, Lui-Roberts WW, Cutler DF. Formation and function of Weibel-Palade bodies. J Cell Sci. 2008; 121:19–27. [PubMed: 18096688]
25. Wagner DD, Mayadas T, Urban-Pickering M, Lewis BH, Marder VJ. Inhibition of disulfide bonding of von Willebrand protein by monensin results in small, functionally defective multimers. J Cell Biol. 1985; 101:112–120. [PubMed: 3924917]
26. Michaux G, et al. The physiological function of von Willebrand's factor depends on its tubular storage in endothelial Weibel-Palade bodies. Dev Cell. 2006; 10:223–232. [PubMed: 16459301]
27. Kabeya Y, et al. LC3, a mammalian homologue of yeast Apg8p, is localized in autophagosome membranes after processing. EMBO J. 2000; 19:5720–5728. [PubMed: 11060023]
28. Komatsu M, Ichimura Y. Physiological significance of selective degradation of p62 by autophagy. FEBS Lett. 2010; 584:1374–1378. [PubMed: 20153326]
29. Klionsky DJ, et al. Guidelines for the use and interpretation of assays for monitoring autophagy in higher eukaryotes. Autophagy. 2008; 4:151–175. [PubMed: 18188003]
30. Jia W, Pua HH, Li QJ, He YW. Autophagy regulates endoplasmic reticulum homeostasis and calcium mobilization in T lymphocytes. J Immunol. 2011; 186:1564–1574. [PubMed: 21191072]
31. Wagner DD. Cell biology of von Willebrand factor. Annu Rev Cell Biol. 1990; 6:217–246. [PubMed: 2275814]
32. Wagner DD, Mayadas T, Marder VJ. Initial glycosylation and acidic pH in the Golgi apparatus are required for multimerization of von Willebrand factor. J Cell Biol. 1986; 102:1320–1324. [PubMed: 3082891]

33. Zenner HL, Collinson LM, Michaux G, Cutler DF. High-pressure freezing provides insights into Weibel-Palade body biogenesis. J Cell Sci. 2007; 120:2117–2125. [PubMed: 17535847]
34. Mijaljica D, Prescott M, Devenish RJ. Endoplasmic reticulum and Golgi complex: Contributions to, and turnover by, autophagy. Traffic. 2006; 7:1590–1595. [PubMed: 17040485]
35. Erent M, et al. Rate, extent and concentration dependence of histamine-evoked Weibel-Palade body exocytosis determined from individual fusion events in human endothelial cells. J Physiol. 2007; 583:195–212. [PubMed: 17540703]
36. Zhou YF, et al. A pH-regulated dimeric bouquet in the structure of von Willebrand factor. EMBO J. 2011; 30:4098–4111. [PubMed: 21857647]
37. Babich V, et al. Selective release of molecules from Weibel-Palade bodies during a lingering kiss. Blood. 2008; 111:5282–5290. [PubMed: 18252862]
38. Alva JA, et al. VE-Cadherin-Cre-recombinase transgenic mouse: a tool for lineage analysis and gene deletion in endothelial cells. Dev Dyn. 2006; 235:759–767. [PubMed: 16450386]
39. Hara T, et al. Suppression of basal autophagy in neural cells causes neurodegenerative disease in mice. Nature. 2006; 441:885–889. [PubMed: 16625204]
40. Komatsu M, et al. Loss of autophagy in the central nervous system causes neurodegeneration in mice. Nature. 2006; 441:880–884. [PubMed: 16625205]
41. Kim JH, Yu YS, Mun JY, Kim KW. Autophagy-induced regression of hyaloid vessels in early ocular development. Autophagy. 2010; 6:922–928. [PubMed: 20818164]
42. Lee SJ, Kim HP, Jin Y, Choi AM, Ryter SW. Beclin 1 deficiency is associated with increased hypoxia-induced angiogenesis. Autophagy. 2011; 7:829–839. [PubMed: 21685724]
43. Kanaji S, Fahs SA, Shi Q, Haberichter SL, Montgomery RR. Contribution of platelet vs. endothelial VWF to platelet adhesion and hemostasis. J Thromb Haemost. 2012; 10:1646–1652. [PubMed: 22642380]
44. Komatsu M, et al. Impairment of starvation-induced and constitutive autophagy in Atg7-deficient mice. J Cell Biol. 2005; 169:425–434. [PubMed: 15866887]
45. Lee IH, et al. Atg7 modulates p53 activity to regulate cell cycle and survival during metabolic stress. Science. 2012; 336:225–228. [PubMed: 22499945]
46. Wu JJ, et al. Mitochondrial dysfunction and oxidative stress mediate the physiological impairment induced by the disruption of autophagy. Aging (Albany NY). 2009; 1:425–437. [PubMed: 20157526]
47. Sirois I, et al. Caspase activation regulates the extracellular export of autophagic vacuoles. Autophagy. 2012; 8:927–937. [PubMed: 22692030]
48. Pallet N, et al. A comprehensive characterization of membrane vesicles released by autophagic human endothelial cells. Proteomics. 2013; 13:1108–1120. [PubMed: 23436686]
49. Johnson R, Charnley J. Hydroxychloroquine in prophylaxis of pulmonary embolism following hip arthroplasty. Clin Orthop Relat Res. 1979:174–177. [PubMed: 535221]

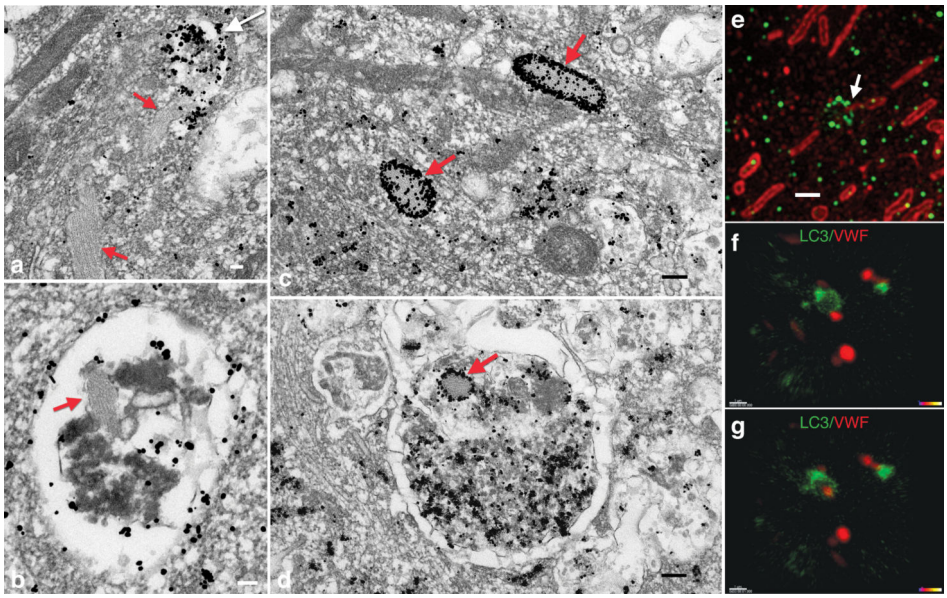

Figure 1.

Proximity of autophagosomes and WPBs within endothelial cells. **a**) Electron micrograph of human endothelial cell demonstrating an LC3 immunogold-labeled autophagosome (white arrow) that is apparently fusing with a WPB (red arrow). White scale bar equals 100 nm. **b**) Tubulated WPB (red arrow) within a LC3 immunogold-labeled autophagosome. **c**) Immunogold-labeled VWF protein within mature WPBs (red arrow). Black scale bar equals 200 nm. **d**) Immunogold detection of VWF protein with mature WPB (red arrow) evident within the autophagosome. **e**) Super resolution structured illumination microscopy of endogenous LC3 (green) and endogenous VWF (red). Arrow demonstrates circular structure decorated with LC3, consistent with an autophagosome, apparently fusing with a cigar shaped VWF-positive WPB. Scale bar equals 1 μm. **f**) Two color live cell imaging of LC3-GFP (green) and VWF-mCherry (red) demonstrating **g)** apparent fusion of these structures in the image obtained one minute later.

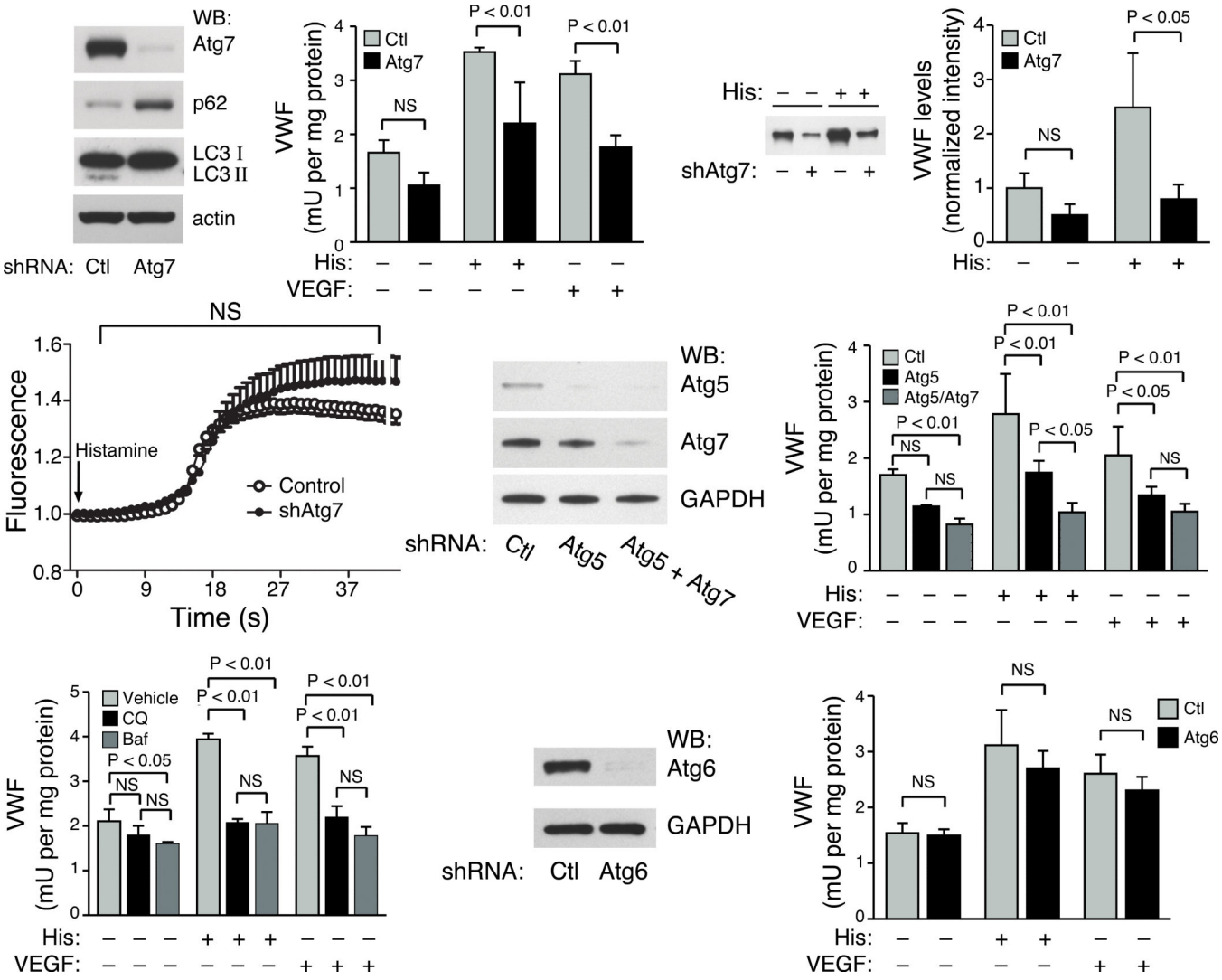

Figure 2.

A role for the essential autophagy proteins Atg5 and Atg7 in endothelial cell secretion of VWF. **a**) Western blot analysis following shRNA mediated knockdown of Atg7 in primary cultures of human endothelial cells for expression of Atg7, p62, LC3 and actin as a loading control. **b**) ELISA of VWF secretion following stimulation with histamine (His) or VEGF. Shown is one representative experiment performed in triplicate. **c**) Western blot analysis of VWF secretion over a 30 minute period in the absence or presence of histamine (His) stimulation. **d**) Quantification of VWF secretion by Western blot analysis (n=4 per condition). **e**) Intracellular calcium imaging using Fluo-4NW relative fluorescence in control shRNA knockdown cells or endothelial cells with Atg7 knockdown. Arrow indicates addition of histamine. **f**) Western blot analysis for Atg5 and Atg7 expression following shRNA mediated knockdown of human endothelial cells. **g**) ELISA measurement of VWF secretion following stimulation with histamine (His) or VEGF for control knockdown cells or following knockdown of Atg5 alone or combined Atg5 and Atg7 knockdown. Shown is one representative experiment performed in triplicate. **h**) Secretion of VWF following

incubation with two known inhibitors of autophagy, chloroquine (CQ) or bafilomycin (Baf). One representative experiment performed in triplicate is shown. **i**) Western blot analysis following shRNA mediated knockdown of Atg6 (beclin-1). **j**) Secretion of VWF following Atg6 knockdown in endothelial cells. Shown is one representative experiment performed in triplicate.

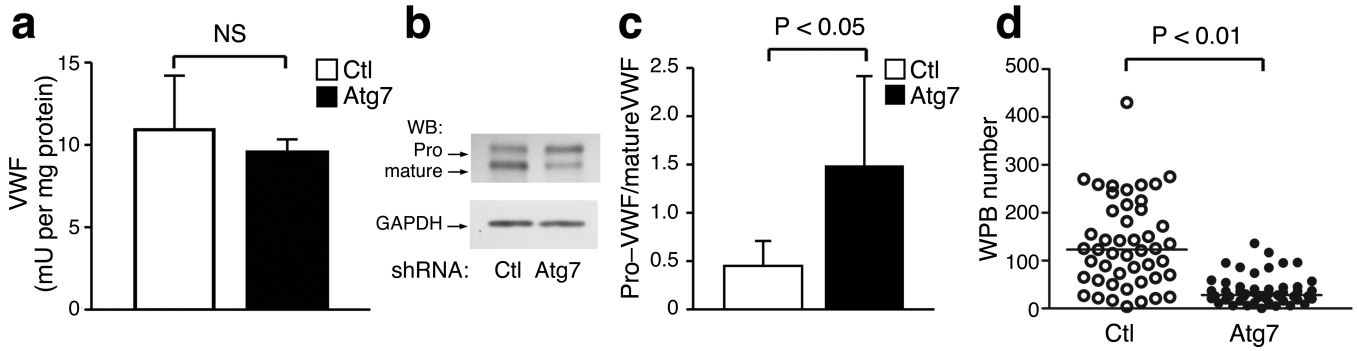

Figure 3.

Atg7 regulates the processing and maturation of VWF. a) Total levels of intracellular VWF protein as measured by quantitative ELISA-based methods (n=3 per sample). **b**) Representative Western blot analysis of intracellular VWF resolving the pro-VWF species from mature VWF protein. **c**) Quantification of the ratio of pro-VWF to mature VWF in endothelial cells with either control or Atg7 shRNA-mediated knockdown. Results are obtained from at least 8 separate Western blots. **d**) Quantification of the number of WPBs per endothelial cell (n>45 cells per condition).

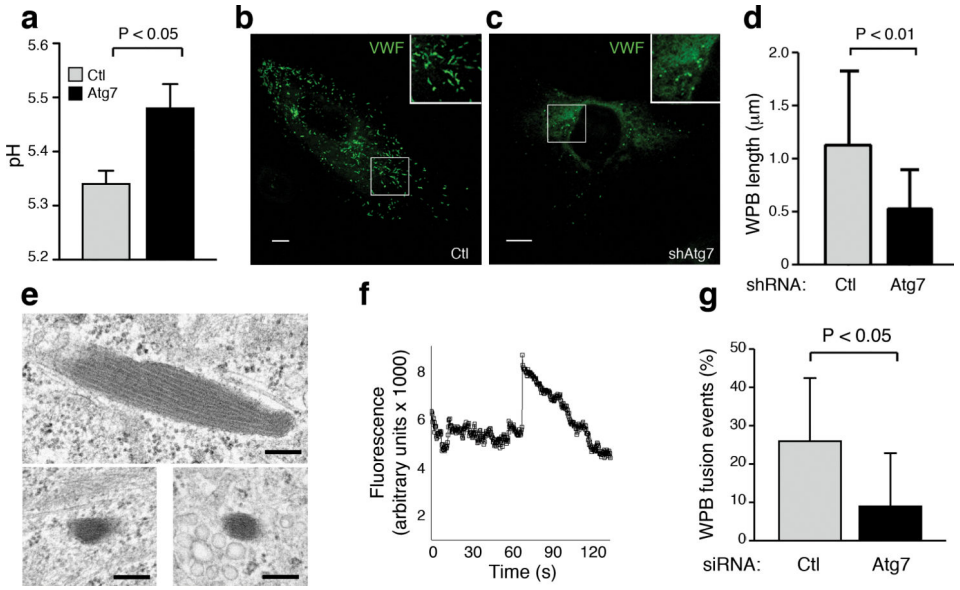

Figure 4.

Autophagy regulates the pH, morphology and secretion of WPBs. **a**) pH determination for WPBs found in control and Atg7 knockdown cells (n=7 for control, n=9 for Atg7 knockdown). **b**) Representative confocal image of WPB morphology in control and **c**) Atg7 knockdown endothelial cells. Insets represent higher power view. Scale bars equal 10 μm. **d**) WPB maximal length measured by confocal microscopy in control (n=277) and Atg7 knockdown cells (n=153). **e**) Electron microscopic image of WPB morphology in control (top panel) or Atg7 knockdown endothelial cells (bottom two panels). Scale bar represents 0.2 μm. **f**) VWF-GFP fluorescent intensity analyzed by TIRF imaging. Histamine was added (t=0) and the sharp spike in intensity approximately 70 seconds later represents an individual secretion event. **g**) Number of VWF-GFP labeled WPBs secreted in control or Atg7 knockdown human endothelial cells (n≥10 per condition). Secretion events recorded were normalized to the total number of WPBs visible in the selected field prior to histamine addition.

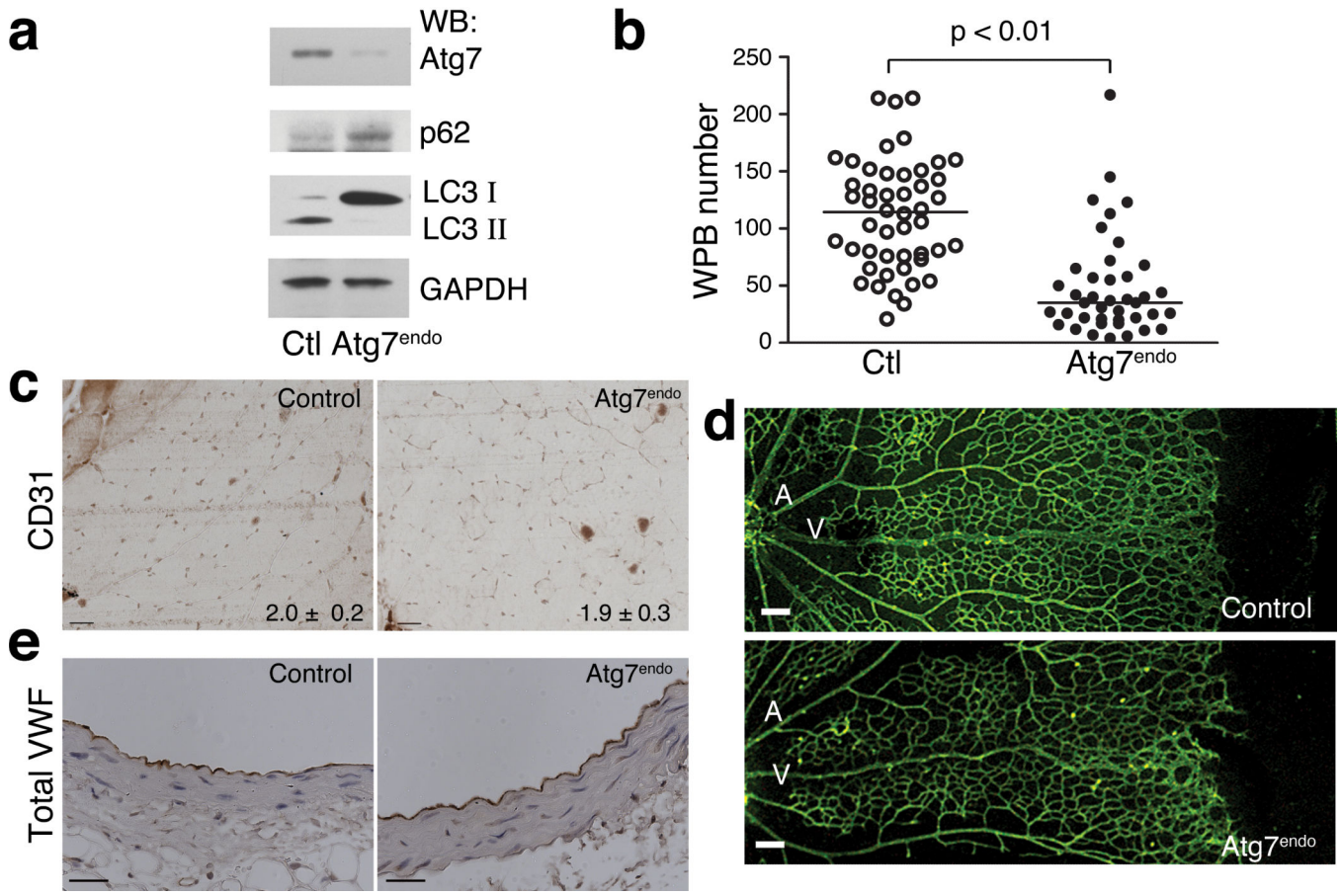

Figure 5.

Conditional endothelial deletion of Atg7 in mice. **a**) Western blot analysis of primary endothelial cells derived from control or Atg7^{endo} mice for expression of Atg7, p62, LC3-I/LC3-II and GAPDH as a loading control. **b**) The number of mature WPBs in endothelial cells obtained from control or Atg7^{endo} mice (n=48 control and n=41 for Atg7^{endo}). **c**) Endothelial cell density in skeletal muscle as assessed by CD31 staining. Numbers at bottom right represents measured ratio of CD31 positive cells to myocytes. Scale bar equals 50 μm. **d**) Neonatal retinal angiogenesis in eight day old control and Atg7^{endo} mice showing retinal artery (A), retinal vein (V) and branching capillaries. Scale bar equals 100 μm. **e**) Representative morphology of aortas from control and Atg7^{endo} mice. Aortic sections are stained for total VWF levels (brown). Scale bar equals 50 μm.

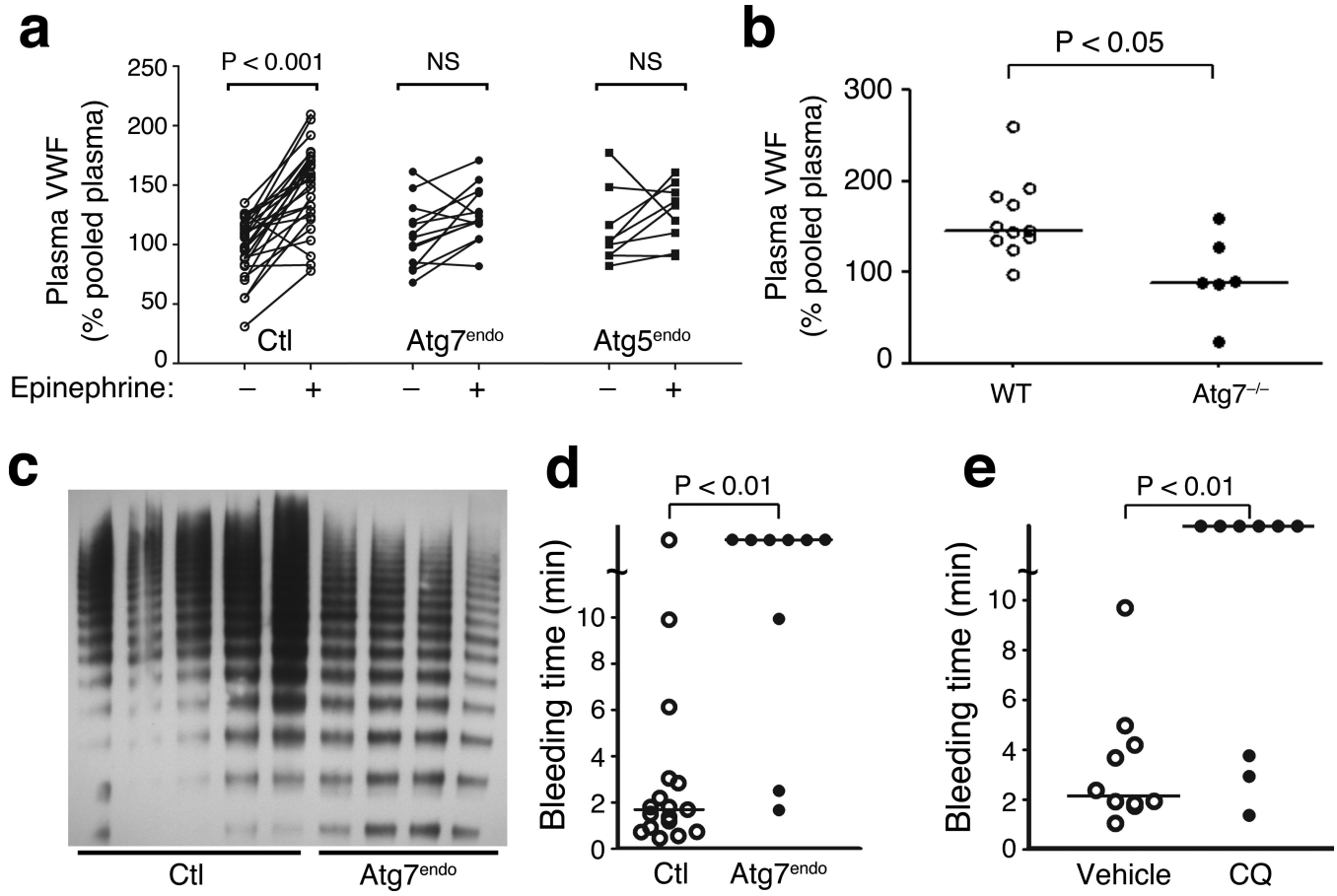

Figure 6.

Inhibition of autophagy alters secretion of VWF in mice. **a**) Plasma levels of VWF in control (n=27), Atg7^{endo} mice (n=13) and Atg5^{endo} mice (n=9) before and after epinephrine injection. Values are expressed relative to the level of VWF obtained from the plasma of five C57BL/6 wild type mice. **b**) Littermates of Atg7$^{+/-}$ parental mice were analyzed on post-natal day one and plasma VWF levels in Atg7$^{+/+}$/WT mice (n=11) and Atg7$^{-/-}$ (n=6) pups were assessed. **c**) Plasma electrophoresis on a non-denaturing and non-reducing gel for VWF multimers in control mice (n=5) and Atg7^{endo} mice (n=4). **d**) Measured bleeding times of individual control (n=17) and Atg7^{endo} mice (n=9). **e**) Measured bleeding time in individual mice treated with vehicle control (n=10) or for 9 days with 60 mg/kg/day of chloroquine (CQ; n=9).